Ultrafast Electric Field-induced Phase Transition in Bulk $Bi_{0.5}Na_{0.5}TiO_3$ under High Intensity Terahertz Irradiation

Man Zhang,[1] Ruth A. McKinnon,[1] Giuseppe Viola,[1] Bin Yang,[2]* Dou Zhang,[3] Michael J. Reece,[1] Isaac Abrahams,[4] and Haixue Yan[1]*

[1] School of Engineering and Materials Science, Queen Mary University of London

London E1 4NS, United Kingdom

[2] Faculty of Science and Engineering, University of Chester

Chester CH2 4NU, United Kingdom

[3] State Key Laboratory of Powder Metallurgy, Central South University

Changsha, Hunan 410083, China

[4] School of Biological and Chemical Sciences, Queen Mary University of London

London E1 4NS, United Kingdom

Keywords: THz pump, THz probe, bismuth sodium titanate, relaxor ferroelectric, ultrafast phase transition

ABSTRACT: Ultrafast polarization switching is being considered for the next generation of ferroelectric based devices. Recently, the dynamics of the field-induced transitions associated with this switching have been difficult to explore, due to technological limitations. The advent of terahertz (THz) technology has now allowed for the study of these dynamic processes on the picosecond (ps) scale. In this paper, intense terahertz (THz) pulses were used as a high-frequency electric field to investigate ultrafast switching in the relaxor ferroelectric, $Bi_{0.5}Na_{0.5}TiO_3$. Transient atomic-scale responses, which were evident as changes in reflectivity, were captured by THz probing. The high energy THz pulses induce an increase in reflectivity, associated with an ultrafast field-induced phase transition from a weakly polar phase (*Cc*) to a strongly polar phase (*R*3*c*) within 20 ps at 200 K. This phase transition was confirmed using X-ray powder diffraction and by electrical measurements which showed a decrease in the frequency dispersion of relative permittivity at low frequencies.

Ferroelectric materials, with switchable electric dipoles, are commonly used as data storage devices,[1-3] piezoelectric actuators,[3] dielectric energy storage,[4] etc. The performance of these ferroelectric-based devices is dependent on the dynamics of the ferroelectric switching, which affects their functionality, for example the operating speed and working temperature.[5] Previous studies of electric field-driven polarization dynamics reported that the switching time of the polarization of oxide films was in the sub-nanosecond time scale.[6] However, these results were largely affected by the rise time of the electrical pulses generated by semiconductor photoconductive switches.[6, 7] One possible way to rapidly manipulate and probe ferroelectric polarization is to use terahertz (THz) pulses. Femtosecond technology has enabled the generation of intense THz pulses with electric fields higher than 100 kV cm^{-1} and time resolutions of around 1 ps.[8,9] Such ultrafast and intense THz pulses make it possible to reveal and manipulate the intrinsic lattice level response. A recent study on the archetypal ferroelectric $BaTiO_3$ (BTO) film,[10] found that large-amplitude rotations of ferroelectric polarization occur on the 10 ps time scale. Similar studies on thin films of $BiFeO_3$[11] and $SrTiO_3$[12], as well as single crystals of the organic ferroelectric tetrathiafulvalene-p-chloranil (TTF-CA),[13] have shown that information on the polarization dynamics can be successfully captured upon intense THz electric field irradiation.

Bismuth sodium titanate ($Bi_{0.5}Na_{0.5}TiO_3$, BNT) is an important ferroelectric with a perovskite-based structure, which has attracted considerable attention in recent years. Functionally, BNT and its derivatives are promising lead-free alternatives to commonly used lead zirconate titanate (PZT)-based piezoelectric ceramics.[14] Physically, BNT is a relaxor ferroelectric and exhibits a sequence of phase transitions during cooling, i.e., from high-temperature cubic to tetragonal structures, and then to rhombohedral and/or monoclinic structures.[15] However, the structure and phase transition behaviour of BNT under ambient conditions are still being debated in the literature.[16-18] Although phase transitions in BNT upon application of a DC bias electric field have been extensively studied, the intrinsic atomic response of BNT is still not resolved.[19] In the present work, we utilise THz pump and THz probe techniques to explore the

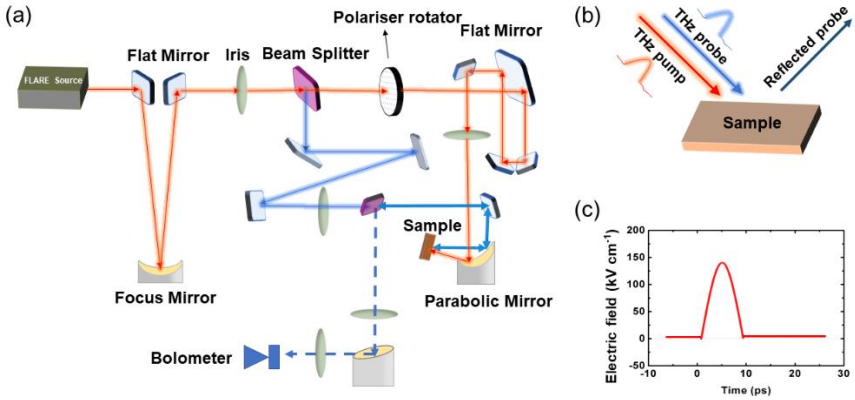

Figure 1. (a) Schematic diagram of THz pump and THz probe system, with detail at the sample position shown in (b) and a plot of electric field generated by a single THz pulse shown in (c). The red arrowed lines represent the THz pump beam and blue arrowed lines denote the THz probe beam. Both the pump and probe beams are optically-focused and overlapped by the parabolic mirror into a spot size of less than 2 mm diameter.

dynamics of ferroelectric polarisation. The intense THz pump was used to manipulate polarization switching, while the THz probe beam was used to inspect the change in reflectivity.

A schematic plot of the THz pump and reflection-based THz probe experimental system is shown in Figure 1a. The THz radiation was generated from a source on the FLARE laser at the FELIX Laboratory in the Netherlands, which was separated into a high-power pump beam and a low power probe beam, using a beam splitter. After travelling along different optical pathways with equal optical lengths, both beams overlap at the sample position. The time zero was taken as the point at which the pump and probe beams had equal optical length; the pump beam was then moved by a submicrometric motor-stage to create an optical path length difference, and this distance variation created the ps time scale for detection of the polarization dynamics. Figure 1b schematically shows the overlapping of THz pump and probe beams on the sample, where the pump beam after irradiating the sample is guided away from the testing system and the THz probe beam is directed to the bolometer detector. In this experiment, the THz pump wave was composed of 60 MHz micro-pulses (i.e. 16.66 ns between pulses), within a 10 s long train that was repeated at 5 Hz. The maximum electric field reaching the sample was about 155 kV cm^{-1}, with a pulse length of about 10 ps, as shown in Figure 1c.

While continuously pumping a high intensity THz beam on the BNT sample, the THz field induced change in reflectivity, ΔR/R, for three continuous THz pump scans was recorded and is shown in Figure 2. Each scan lasted around 30 min, during which the sample was continuously irradiated. At the end of each scan, the pump beam position was returned to that at time zero. As BNT exhibits high dielectric loss at room temperature, the experiment was performed at 200 K to minimize conductivity losses. Higher values of ΔR/R are indicative of high dielectric permittivity in the material at THz frequencies.[20] There is a sharp increase in the relative reflectivity of BNT after 20 ps THz pump irradiation. The higher reflectivity indicates an increase in permittivity, consistent with a phase transition from a weak polar structure to a strong polar structure. The increasing reflectivity of the sample with time indicates an increased fraction of the strong polar phase. The continuous increase in reflectivity, suggests that the duration of the THz irradiation at 200 K (ca. 30 min per scan = 1.5 h) was insufficient to completely transform the sample.

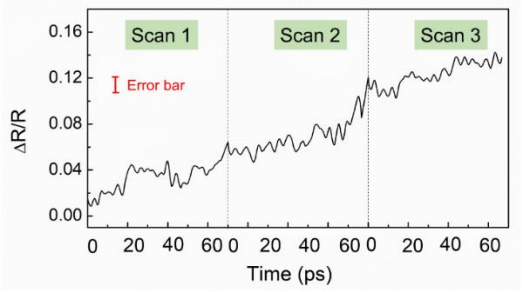

Figure 2. Time evolution of ΔR/R under three continuous 1.36 THz (45 cm^{-1}) pump-probe scans at 200 K.

Figure 3 shows a comparison of the (110) perovskite peak in the room temperature XRD patterns of unpoled (U-BNT), THz-pumped (T-BNT) and, DC-poled (DC-BNT) BNT samples. It is evident that a significant change occurs on THz pumping, which is further accentuated in the pattern after DC poling. The fitted diffraction profiles of U-BNT, T-BNT and DC-BNT samples are given in the supporting information as Figure S1-S3. Crystal and refinement data are summarised in Table 1. The structure of the unpoled sample can be described in the monoclinic space group *Cc*;[19, 21] the refined structural parameters for this phase in U-BNT are given in Table S1. On DC poling, a field induced transition to the rhombohedral phase in space group *R*3*c* occurs, consistent with literature reports.[18, 19] Rietveld analysis of the unpoled and poled data confirm 86 wt% conversion to the rhombohedral phase post DC poling. The field that occurs in the THz pumping experiment also results in a field induced transition, but is less extensive than in the DC poling experiment, due to the short duration of pulses and lower temperature (200 K) of the THz pumping experiment, with only 45 wt% conversion. Similar changes in BNT after poling under different electric field were reported by Badari et al..[18] Thus, BNT is irreversibly transformed from the monoclinic

Table 1 Crystal and Refinement parameters for U-BNT, T-BNT and DC-BNT samples. Estimated standard deviations are given in parentheses.

	U-BNT	T-BNT	DC-BNT
Phase 1			
Crystal system	Monoclinic	Monoclinic	Monoclinic
Space group	*Cc*	*Cc*	*Cc*
Formula weight	211.88 g mol^{-1}	211.88 g mol^{-1}	211.88 g mol^{-1}
Unit cell dimensions	a = 9.4949(9) Å	a = 9.506(1) Å	a = 9.548(1) Å
	b = 5.4790(4) Å	b = 5.4819(3) Å	b = 5.4731(8) Å
	c = 5.5153(5) Å	c = 5.5145(6) Å	c = 5.5137(8) Å
	β = 125.181(5)°	β = 125.091(8)°	β = 125.101(9)°
Volume	234.51(2) Å^3	235.15(4) Å^3	235.73(3) Å^3
Z	4	4	4
Density (calculated)	6.001 g cm^{-3}	5.985 g cm^{-3}	5.970 g cm^{-3}
Wt Fraction	1	0.453(9)	0.131(5)
Phase 2			
Crystal system		Trigonal	Trigonal
Space group		*R*3*c*	*R*3*c*
Formula weight		211.88 g mol^{-1}	211.88 g mol^{-1}
Unit cell dimensions		a = 5.515(1) Å	a = 5.47962(8) Å
		c = 13.531(4) Å	c = 13.5641(2) Å
Volume		356.4(2)Å^3	352.71(1) Å^3
Z		6	6
Density (calculated)		5.922 g cm^{-3}	5.985 g cm^{-3}
Wt Fraction		0.547(14)	0.869(3)
R-factors[a]	R_{wp} = 0.1038	R_{wp} = 0.0833	R_{wp} = 0.0928
	R_p = 0.0805	R_p = 0.0661	R_p = 0.0716
	R_{ex} = 0.0778	R_{ex} = 0.0618	R_{ex} = 0.0618
	R_F^2 = 0.1896	R_F^2 = 0.2808	R_F^2 = 0.1586
	χ^2 = 1.788	χ^2 = 1.537	χ^2 = 2.270
No. of variables[b]	38	43	30
No of profile points used	6582	3140	6582
No of reflections	366	496	494

[a] For definition of R-factors see reference[27]

[b] Additional spherical harmonics variables to account for preferred orientation in T-BNT sample. Atomic parameters were refined in the analysis of the single phase U-BNT sample but not in the multiphase samples.

to the rhombohedral phase on application of an electric field, using either THz radiation or normal DC bias. Increased distortion of the monoclinic phase (evidenced by an increase in volume) is seen in the T-BNT and DC-BNT samples, with the distortion greatest in the latter. Similarly, distortion of the rhombohedral phase (evidenced by an increase in the c/a ratio) is greatest in the DC-BNT sample.

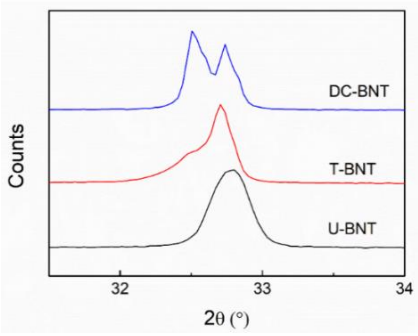

Figure 3. (110) perovskite reflection in XRD patterns of unpoled (U-BNT), THz-pumped (T-BNT) and, DC-poled (DC-BNT) BNT samples.

Another difference between the three BNT samples was found in the degree of their dielectric dispersions at low frequency (below 1 MHz). Figure 4 shows the dielectric permittivity of the three BNT samples as a function of frequency. As can be seen, the permittivity of the three samples decreases linearly with log frequency. The slope of the linear plot, α, which is calculated from the following relationship:

$$\varepsilon' = \varepsilon'_0 - \alpha log f \qquad (1)$$

can be used to quantify the frequency dispersion.[16, 22, 23] The slopes for the T-BNT and DC-BNT samples have nearly the same α-value, being a quarter that of the U-BNT sample (-33.1). The strong dielectric relaxation in the unpoled BNT is due to the lack of long-range polarization in the monoclinic phase.[16] It is worth noting that the high dielectric permittivity value of the unpoled BNT sample, in the low frequency range, is also related to a high density of ferroelectric domain walls, which are not active at THz frequencies.[24, 25] The decreased dielectric relaxation in T-BNT and DC-BNT samples indicates that these samples exhibit greater long-range

structural coherence, which is a consequence of field induced transitions. As discussed above, the structure in unpoled BNT exhibits *Cc* symmetry, which has a lower phase stability than the rhombohedral (*R*3*c*) phase under applied electric field. Upon intense THz pump illumination, the fraction of the less stable *Cc* structure in BNT is reduced as the structure transforms to *R*3*c* symmetry. Recent experimental results on THz probing show that a DC field induced transition in BNT-based ceramics is linked to an increase in dielectric permittivity at THz frequencies.[26] This is consistent with our observation of a THz radiation induced phase transition from weak to strong polar phases, leading to increased dielectric permittivity at THz frequencies (Figure 2). The overall change in ΔR/R seen in Figure 2 is relatively small, consistent with only a partial transition from *Cc* to *R*3*c* structures.

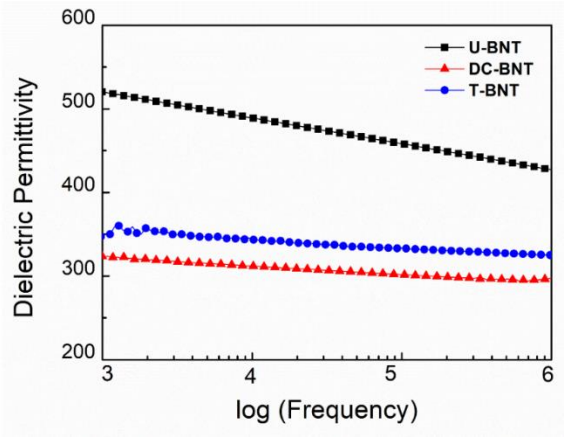

Figure 4. Frequency variation of relative permittivity in the studied BNT samples.

In summary, the electric field driven phase transition in BNT ceramic was successfully captured by the high energy THz pump and probe measurement. The high energy THz pump induced an ultrafast phase transition from weak polar (*Cc*) to strong polar (*R*3*c*) phases within 20 ps at 200 K. The work demonstrates that BNT could be applied for new devices based on ultrafast field induced transitions. The THz pump and probe methodology presented here opens an interesting new pathway to probe the dynamics of ultrafast phase transitions in ferroelectrics, which are related to changes in polarization. This is fundamental to the operation ferroelectric based devices and is key to the development of next-generation piezoelectric, electrocaloric, electro-optic devices as well as non-volatile memories and sensors.

ASSOCIATED CONTENT

Supporting Information.

Experimental procedures, XRD results and refined data are included in the supporting information. This material is available free of charge via the Internet at http://pubs.acs.org.

AUTHOR INFORMATION

Corresponding Authors

*Haixue Yan, School of Engineering and Materials Science, Queen Mary University of London, London E1 4NS, United Kingdom. Email: h.x.yan@qmul.ac.uk

*Bin Yang, Faculty of Science and Engineering, University of Chester, Chester CH2 4NU, United Kingdom. Email: b.yang@chester.ac.uk

Present Addresses

†If an author's address is different than the one given in the affiliation line, this information may be included here.

Author Contributions

M.Z. and R.A.M. produced samples and carried out the structure and dielectric measurements. M.Z. prepared the first manuscript with basic interpretation. G.V., B.Y., D.Z., M.J.R and I.A. contributed to the analysis of structures and properties. B.Y. carried out the THz measurement. B.Y., I.A and H.Y. initiated and mentored the work. All authors contributed to the preparation of the manuscript. All authors have given approval to the final version of the manuscript.

Notes

The authors declare no conflict of interest.

ACKNOWLEDGMENT

This work was supported by the EPSRC (MASSIVE project, EP/L017695/1; 1157398; FLUENCE project, EP/R007926/1) and funding from the China Scholarship Council (CSC, 201706370172). The use of the FLARE source was supported by FELIX Laboratory.

ABBREVIATIONS

$Bi_{0.5}Na_{0.5}TiO_3$, BNT

REFERENCES

(1) Jiang, A. Q.; Lee, H. J.; Hwang, C. S.; Scott, J. F. Sub-picosecond Processes of Ferroelectric Domain Switching from Field and Temperature Experiments. *Adv. Funct. Mater*. **2012**, *22*, 192–199.

(2) Grinberg, I.; Shin, Y. H.; Rappe, A. M. Molecular Dynamics Study of Dielectric Response in a Relaxor Ferroelectric. *Phys. Rev. Lett*. **2009**, *103*, 197601.

(3) Liu, Y.; Wang, Q. Ferroelectric Polymers Exhibiting Negative Longitudinal Piezoelectric Coefficient: Progress and Prospects. *Adv. Sci*. **2020**, *7*, 1902468.

(4) Wu, J.; Zhang, H.; Huang, C.-H.; Tseng, C.-W.; Meng, N.; Koval, V.; Chou, Y.-C.; Zhang, Z.; Yan, H. Ultrahigh Field-induced Atrain in Lead-free Ceramics. *Nano Energy* **2020**, *76*, 105037.

(5) Rana, D. S.; Kawayama, I.; Mavani, K.; Takahashi, K.; Murakami, H.; Tonouchi, M. Understanding the Nature of Ultrafast Polarization Dynamics of Ferroelectric Memory in the Muitiferroic $BiFeO_3$. *Adv. Mater*. **2009**, *21*, 2881–2885.

(6) Li, J.; Nagaraj, B.; Liang, H.; Cao, W.; Lee, C. H.; Ramesh, R. Ultrafast Polarization Switching in Thin-film Ferroelectrics. *Appl. Phys. Lett*. **2004**, 84, 1174–1176.

(7) Li, J.; Liang, H.; Nagaraj, B.; Cao, W.; Lee, C. H.; Ramesh, R. Application of An Ultrafast Photonic Technique to Study Polarization Switching Dynamics of Thin-film Ferroelectric Capacitors. *J. Light. Technol*. **2003**, *21*, 3282–3291.

(8) Hirori, H.; Doi, A.; Blanchard, F.; Tanaka, K. Single-cycle Terahertz Pulses with Amplitudes Exceeding 1 MV/cm Generated by Optical Rectification in $LiNbO_3$. *Appl. Phys. Lett*. *2011*, *98*, 091106.

(9) Morimoto, T.; Miyamoto, T.; Yamakawa, H.; Terashige, T.; Ono, T.; Kida, N.; Okamoto, H. Terahertz-Field-Induced Large Macroscopic Polarization and Domain-Wall Dynamics in an Organic Molecular Dielectric. *Phys. Rev. Lett*. **2017**, *118*, 107602.

(10) Chen, F.; Zhu, Y.; Liu, S.; Qi, Y.; Hwang, H. Y.; Brandt, N. C.; Lu, J.; Quirin, F.; Enquist, H.; Zalden, P.; Hu, T.; Goodfellow, J.; Sher, M.-J.; Hoffmann, M. C.; Zhu, D.; Lemke, H.; Glownia, J.; Chollet, M.; Damodaran, A. R.; Park, J.; Cai, Z.; Jung, I. W.; Highland, M. J.; Walko, D. A.; Freeland, J. W.; Evans, P. G.; Vailionis, A.; Larsson, J.; Nelson, K. A.; Rappe, A. M.; Sokolowski-Tinten, K.; Martin, L. W.; Wen, H.; Lindenberg, Ultrafast Terahertz-field-driven Ionic Response in Ferroelectric $BaTiO_3$. A. M. *Phys. Rev. B* **2016**, *94*, 180104.

(11) Chen, F.; Goodfellow, J.; Liu, S.; Grinberg, I.; Hoffmann, M. C.; Damodaran, A. R.; Zhu, Y.; Zalden, P.; Zhang, X.; Takeuchi, I.; Rappe, A. M.; Martin, L. W.; Wen, H.; Lindenberg, A. M. Ultrafast Terahertz Gating of the Polarization and Giant Nonlinear Optical Response in $BiFeO_3$ Thin Films. *Adv. Mater.* **2015**, *27*, 6371–6375.

(12) Katayama, I.; Aoki, H.; Takeda, J.; Shimosato, H.; Ashida, M.; Kinjo, R.; Kawayama, I.; Tonouchi, M.; Nagai, M.; Tanaka, K. Ferroelectric Soft Mode in a $SrTiO_3$ Thin Film Impulsively Driven to the Anharmonic Regime Using Intense Picosecond Terahertz Pulses. *Phys. Rev. Lett*. **2012**, *108*, 097401.

(13) Miyamoto, T.; Yada, H.; Yamakawa, H.; Okamoto, H. Ultrafast Modulation of Polarization Amplitude by Terahertz Fields in Electronic-type Organic Ferroelectrics. *Nat. Commun*. **2013**, *4*, 1–9.

(14) Rödel, J.; Jo, W.; Seifert, K. T. P.; Anton, E. M.; Granzow, T.; Damjanovic, D. Perspective on the Development of Lead-free Piezoceramics. *J. Am. Ceram. Soc*. **2009**, *92*, 1153–1177.

(15) Jones, G. O.; Thomas, P. A. Investigation of the Structure and Phase Transitions in the Novel A-site Substituted Distorted Perovskite Compound $Na_{0.5}Bi_{0.5}TiO_3$. *Acta Crystallogr. Sect. B Struct. Sci*. **2002**, *58*, 168–178.

(16) Rao, B. N.; Datta, R.; Chandrashekaran, S. S.; Mishra, D. K.; Sathe, V.; Senyshyn, A.; Ranjan, R. Local Structural Disorder and Its Influence on the Average Global Structure and Polar Properties in $Na_{0.5}Bi_{0.5}TiO_3$. *Phys. Rev. B* **2013**, *88*, 224103.

(17) Beanland, R.; Thomas, P. A. Symmetry and Defects in Rhombohedral Single-crystalline $Na_{0.5}Bi_{0.5}TiO_3$. *Phys. Rev. B - Condens. Matter Mater. Phys*. **2014**, *89*, 174102.

(18) Rao, B. N.; Fitch, A. N.; Ranjan, R. Ferroelectric-ferroelectric Phase Coexistence in $Na_{1/2}Bi_{1/2}TiO_3$. *Phys. Rev. B*. **2013**, *87*, 060102.

(19) Rao, B. N.; Ranjan, R. Electric-field-driven Monoclinic-to-rhombohedral Transformation in $Na_{1/2}Bi_{1/2}TiO_3$. *Phys. Rev. B*. **2012**, *86*, 134103.

(20) Lee, C. H.; Orloff, N. D.; Birol, T.; Zhu, Y.; Goian, V.; Rocas, E.; Haislmaier, R.; Vlahos, E.; Mundy, J. A.; Kourkoutis, L. F.; Nie, Y.; Biegalski, M. D.; Zhang, J.; Bernhagen, M.; Benedek, N. A.; Kim, Y.; Brock, J. D.; Uecker, R.; Xi, X. X.; Gopalan, V.; Nuzhnyy, D.; Kamba, S.; Muller, D. A.; Takeuchi, I.; Booth, J. C.; Fennie, C. J.; Schlom, D. G. Exploiting Dimensionality and Defect Mitigation to Create Tunable Microwave Dielectrics. Nature **2013**, *502*, 532–536.

(21) Gorfman, S.; Thomas, Evidence for a Non-rhombohedral Average Structure in the Lead-free Piezoelectric Material $Na_{0.5}Bi_{0.5}TiO_3$. P. A. *J. Appl. Crystallogr*. **2010**, *43*, 1409–1414.

(22) Jin L. Broadband Dielectric Response in Hard and Soft PZT : Understanding Softening and Hardening Mechanisms. THESIS, EPFL, **2011**.

(23) Viola, G.; Ning, H.; Wei, X.; Deluca, M.; Adomkevicius, A.; Khaliq, J.; John Reece, M.; Yan, H. Dielectric Relaxation, Lattice Dynamics and Polarization Mechanisms in $Bi_{0.5}Na_{0.5}TiO_3$-based Lead-free Ceramics. J. *Appl. Phys*. **2013**, *114*, 014107.

(24) Hoshina, T.; Kigoshi, Y.; Hatta, S.; Teranishi, T.; Takeda, H.; Tsurumi, T. Size Effect and Domain-wall Contribution of Barium Titanate Ceramics. *Ferroelectrics* **2010**, *402*, 29–36.

(25) Tsurumi, T.; Li, J.; Hoshina, T.; Kakemoto, H.; Nakada, M.; Akedo, Ultrawide Range Dielectric Spectroscopy of $BaTiO_3$-based Perovskite Dielectrics. *J. Appl. Phys. Lett*. **2007**, *91*, 182905.

(26) Wu, J.; Sun, W.; Meng, N.; Zhang, H.; Koval, V.; Zhang, Y.; Donnan, R.; Yang, B.; Zhang, D.; Yan, H. Terahertz Probing Irreversible Phase Transitions Related to Polar Clusters in Bi0.5Na0.5TiO3-Based Ferroelectric. *Adv. Electron. Mater*. **2020**, *6*, 1901373.

(27) Goldberg, A. E. GSAs. *Rep. lAUR* **1994**, 686-748.

For Table of Contents Use Only

Ultrafast Electric Field-induced Phase Transition in Bulk $Bi_{0.5}Na_{0.5}TiO_3$ under High Intensity Terahertz Irradiation

Man Zhang, Ruth A. McKinnon, Giuseppe Viola, Bin Yang,* Dou Zhang, Michael J. Reece, Isaac Abrahams, and Haixue Yan*

Intense terahertz (THz) pulses, which act as a high frequency electric field induce an ultrafast phase transition from the weakly polar monoclinic (*Cc*) phase to the strongly polar rhombohedral (*R*3*c*) phase in $Bi_{0.5}Na_{0.5}TiO_3$ within 20 ps at 200K.